Modeling, Identification and Prediction of Inherent quasi-stationary Pressure Dynamics of a Common-Rail System using Neuro-Fuzzy Structures with Local Linear ARX models

Gelu Laurenţiu Ioanaş

"Politehnica" University of Timişoara, Faculty of Automation and Computer Science, Romania
Continental Automotive Timisoara, Powertrain Engine Systems.
e-mail: gelu.ioanas@continental-corporation.com

Abstract: In the opening there is a short overview for the current approaches found in the literature regarding the methods and models used for the Common Rail diesel high pressure dynamics identification. The local linear Neuro-Fuzzy models are proposed as an alternative to the conventional analytical and empirical models. In the following, the diesel Common Rail system structure is presented along with the basic physical equations governing the process. A short analysis reveals the main factors influencing the fuel pressure behavior inside the Common Rail high pressure system. Finally, it is analyzed the feasibility for the high pressure system identification and modeling using a particular Neuro-Fuzzy network structure with local linear dynamic models by training its parameters with engine measured data.

Keywords: Diesel engines, pressure, identification, local, Neural-network models, adaptive, parameter estimation.

1. INTRODUCTION

Modeling complex technological processes in detail using theoretical methods and implementing the resulting analytical models in a real time computing environment requires an elaborate work and it's time consuming. These aspects are most relevant when referring to the automotive industry, where the mechanical and thermo-dynamical processes are interconnected and the identification methods represent an alternative for obtaining empirical process models with limited validity regions. In numerous applications, the Neuro - Fuzzy networks have demonstrated their capability to provide nonlinear models directly from the measured data, without necessity for detailed knowledge of the strong nonlinear processes (Hafner et al. (2002), p. 402-412).

1.1 Motivation

In the past years, the auto industry had seen a considerable progress and the biggest automotive manufactures along with their technical solutions suppliers had implemented various methods and design architectures with the purpose to satisfy the customer requirements and reduce development costs. In order to get the right picture over the degree of difficulty associated with the automotive projects, one needs to integrate them into a strong competitive environment with tight deadlines which emerged after the 2009 financial crisis. The projects related to the Common Rail injection systems make no exception and follow the same philosophy: on one hand, achieving the emission related objectives (EU6, EU7, SULEV), on the other, reducing cost and time to market (Continental (2009a)).

The above outlined aspects impose the need for an open system architecture (AUTOSAR - AUTomotive Open System ARchitecture), which allows the engine manufactures to chose various suppliers for different components which minimize the cost vs. performance criteria. The resulted systems are characterized by functional complexity and inherit new characteristics difficult to be reproduced by the already existing models based on analytical equations and/or numerical dependencies implemented via look-up tables. From the newly raised constraints, emerges the necessity for implementing new model structures and appropriate identification algorithms capable to adapt the parameters off and on-line for the entire engine workspace, with the designated purpose to compensate the inaccuracy of old models or even replace them. An extra argument for choosing an adaptive model structure is represented by the time varying characteristics of the systems which lead to a drop in the model accuracy over time. A model based control structure, without a systematic parameter adaptation, is not capable to keep the original system performances over its lifetime.

1.2 Current approaches for Common Rail fuel pressure system identification and modeling

The technical literature doesn't exceed in publication referring to identification methods and numerical models used to approximate the fuel pressure behaviour inside the Common Rail systems. Continental, Bosch and Delphi, the major suppliers of control systems for Common Rail diesel injection, had decided to patent the technological solutions

without making public the theoretical content of the implemented applications. This comes rather logical, taking into account that in the past years the three rivals competed for reducing the Common Rail diesel engine emissions and improving its performances (Continental (2009), Yldiz (2009), Delphi (2009)).

There can be found in the technical literature some papers describing analytical methods for identification and modeling of the Common Rail fuel pressure behaviour. Lino, Maione and (Rizzo (2007)) propose a Common Rail injection system model using the state space which is further used for designing a sliding mode pressure controller. The resulted model is validated against measurements and the control structure performances are evaluated using AMESim and Matlab. In a different paper (Lino et al. (2008)), a parametrical identification method (ARIX) is presented and this time for modeling the gas pressure in a modified Common Rail natural gas injection system. The identification results are crystallized into a model used for predictive control of the gas pressure inside the injection system. The model validation on an experimental test bench, demonstrates the potential of the model based predictive control structure versus a conventional one.

Several papers include detailed observations on different components of the high pressure system along with the important factors influencing the fuel pressure dynamics. (Zeilang Li (2005)) performs an analysis on the high pressure fuel pump with the purpose of extracting an analytical model, validated experimentally, which approximates the shape of the fuel pressure waves generated by the pump. The fuel bulk modulus of elasticity (E) used in the calculation represents one of the most significant factors for the fuel flow model in a common-rail volume V and implicitly has a great influence on the fuel pressure (P).

$$E = -V \cdot \frac{dP}{dV} \tag{1}$$

(Seykens *et. al.* (2004) and Boudy *et. al*. (2009)) formulate, after summarizing the experiments, conclusions over the influence of the biodiesel fuels properties upon the common rail fuel pressure systems. Again, the damping of the fuel pressure waves is directly linked to the fuel bulk modulus of elasticity. In his study, (Kiijarvi (2003)) provides detailed analytical models of the fuel flow and pressure for all Common-Rail system components.

The correlation between the high pressure system pressure pulsations and the engine rotational angle was investigated by (Zhang and Sun (2009)). An angle-varying dynamic model was developed to model the system dynamics and especially the pressure pulsations introduced by the high pressure pump. In order to leverage the periodicity of pulsations in rotational-angle domain, they designed a piezo driven actuator capable to absorb and provide high pressure and high speed flow in real time. An internal model-based controller was designed as well for the actuator control.

In conclusion, common rail fuel pressure modeling and predictive control are topics of interest among the scientific community. There can be found studies where global approaches are applied for approximating the behaviour for the overall common rail fuel pressure system or studies focused on particular aspects of the system but in despite of that, there is no solution capable to provide a real time prediction of the common rail fuel pressure dynamics with a deviation from the real value under 1~2 MPa for the entire engine working space. This restrictive constraint calls for an alternative approach in designing a model capable to fulfill the task of adapting it's parameters from system data around quasi-stationary engine working points and then perform the prediction of common rail fuel pressure over a certain time horizon.

The next sections of this paper are focusing on the Common Rail fuel pressure system particularities and offer an alternative to the classic approaches for identification and modeling. In chapter II, the local linear Neuro-Fuzzy models are proposed as an alternative to the conventional analytical and empirical models. In the following, the diesel Common Rail system structure is presented along with the basic physical equations governing the process. Chapter III, reveals the main factors influencing the fuel pressure behavior inside the common rail high pressure system. Chapter IV, presents a high pressure system identification and modeling using a particular Neuro-Fuzzy network structure with local linear dynamic models. The resulted application is designed to adapt its parameters and then predict the common rail pressure for a specific engine working point. The parameters training is performed with engine measured data and the simulation results are analyzed.

2. PROPOSED METHOD FOR SYSTEM MODELING AND PARAMETERS IDENTIFICATION

A. Modeling and identification using local linear Neuro-Fuzzy networks

Various approaches on modeling and identification methods based on Neuro-Fuzzy network architectures can be found in the literature. This paper will focus on a particular architecture with local linear dynamic models and the associated identification algorithm.

Starting from an idea initially promoted by (Murray (1994), Nelles *et al.* (1996, 2000)) introduced the LOLIMOT (Local Linear Model Tree) concept based on RBF (Radial Basis Function) Neuro-Fuzzy networks with local linear models (LLMs). The LOLIMOT construction algorithm combines the heuristic method of decomposing the input space with the local optimization based on the least- squares technique. After the input space decomposition in an axis – orthogonal manner, the resulted (hyper-) rectangles have centers which coincide with the centers of Gaussian membership functions. The standard deviation for the membership functions are chosen to be proportional with the (hyper-) rectangles dimensions, taking into account the varying granularity. In this way, explicit nonlinear optimization is avoided and the nonlinear parameters are determined heuristically (Nelles et al. (2000)). The solution requires a moderate computational effort (Nelles (2001)). The concept was tested in the automotive field and its potential was demonstrated in several multivariable nonlinear applications: feed forward ignition

angle control, modeling the charging process of a Diesel engine by an exhaust turbocharger (Nelles (2001)). (Jakubek and Keuth ((2006)) apply the LOLIMOT concept for modeling and parameter optimization of Diesel engine combustion process.

B. Local Linear Neuro-Fuzzy models structure

(Nelles and Fischer ((1996)) present a practical solution for using Neuro – Fuzzy networks in process modeling and identification. Dynamic MISO models with $r+1$ inputs, u_1, ..., u_r, y, represented by the NARX structure:

$$\hat{y}_{pg} = f\begin{pmatrix} u_1(k-1),\ldots,u_1(k-n_{u_1}),\ldots, \\ u_r(k-1),\ldots,u_r(k-n_{u_r}) \\ y(k-1),\ldots,y(k-n_y) \end{pmatrix} \quad (2)$$

can be easily identified using LOLIMOT algorithm. The global predicted output $\hat{y}_{pg}$ is determined as a function of the input vector u and measured output y.

Having as objective empirical process modeling for predictive control, the Neuro – Fuzzy network architecture structured on two levels presented in fig. 1 is considered (Nelles (2000)). From *a priori* expert knowledge of the process, the ensemble of input vector $\underline{u}$ measured output y generates after some preliminary operation the neuron's inputs $\underline{z} = [z_1, \ldots, z_{nz}]^T$, and $\underline{x} = [x_1, \ldots, x_{nx}]^T$. This operation is called *selection*.

The network structure consists of M neurons (Fig.1) whose outputs $\hat{y}_i$, $i = 1, \ldots, M$, provide the predicted output $\hat{y}_{pg}$ according to formula (3). The formula corresponds to a Tagaki-Sugeno processing level (Level 1 in Fig. 1a) for which the validity functions $\Phi_i(\underline{z})$ bring the rule premise:

$$\hat{y}_{pg} = \sum_{i=1}^{M} \hat{y}_{pi}(\underline{x}, z', \underline{z}) = \sum_{i=1}^{M} \hat{y}_i(\underline{x}, z') \cdot \Phi_i(\underline{z}) \quad (3)$$

Each term $\hat{y}_i(\underline{x}, z')$, i =1, …, M from first level, represents the output of a local model, LM_i which further consist, on the second level (Level 2 in Fig. 1b), in n local linear sub-models (LLMs) that implement dependencies of the form:

$$\hat{y}_i(\underline{x}, z') = w_{i,0} + \sum_{j=1}^{n} \hat{y}_{i,j}(\underline{x}) \cdot \Phi'_{i,j}(z') = w_{i,0} + \sum_{j=1}^{n} \underline{w}_{i,j}(\circ)\underline{x} \cdot \Phi'_{i,j}(z') \quad (4)$$

Here $\underline{w}_{i,j}(o) = [w_{i,0}(o), w_{i,j,1}(o), \ldots, w_{i,j,nx}(o)]$ is the vector of the weighting operators, and $\Phi'_{i,j}(z')$ represent the validity functions depending on a third selected input: z'. In equation (4), each LM represents also a Tagaki-Sugeno rule. Details about the processing are presented further in chapter IV.

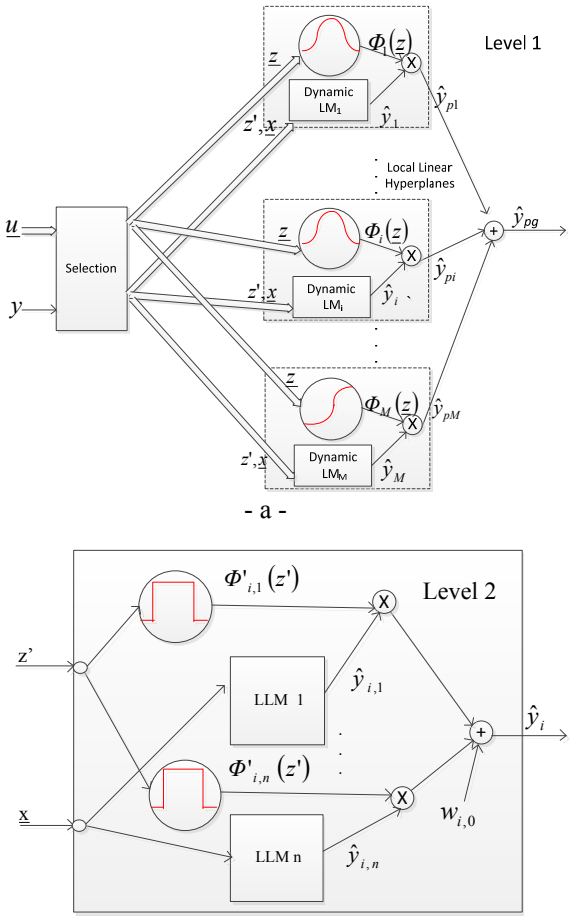

- a -

- b -

Fig. 1. Neuro – Fuzzy network structure with local dynamic models, having on first level M neurons for n_x consequent inputs x and n_z premise inputs z for the 1st level validity functions (fig.1a) and each neuron having a network structure with n local linear models, n_x consequent inputs x and a premise input z' for the 2nd level validity functions (fig.1b).

3. COMMON-RAIL HIGH PRESSURE SYSTEM

In the following, a 3 piston pump and 4 injectors Piezo Common-rail system (PCR) is considered. According to (Lino et al. (2007), Continental (2009b) and Wikipedia (2012)) the PCR configuration presented in fig. 2 can be considered as one of the last generation. The main circuits of the hydraulic system are the low pressure circuit (bottom) and the high pressure circuit (top). The first circuit contains the low pressure pump which lifts the fuel pressure from the tank, the internal transfer pump and the fuel return line with the fuel temperature sensor, whereas the second one contains the high pressure pump the volumetric and pressure control valves, the common rail together with the fuel pressure sensor and injectors.

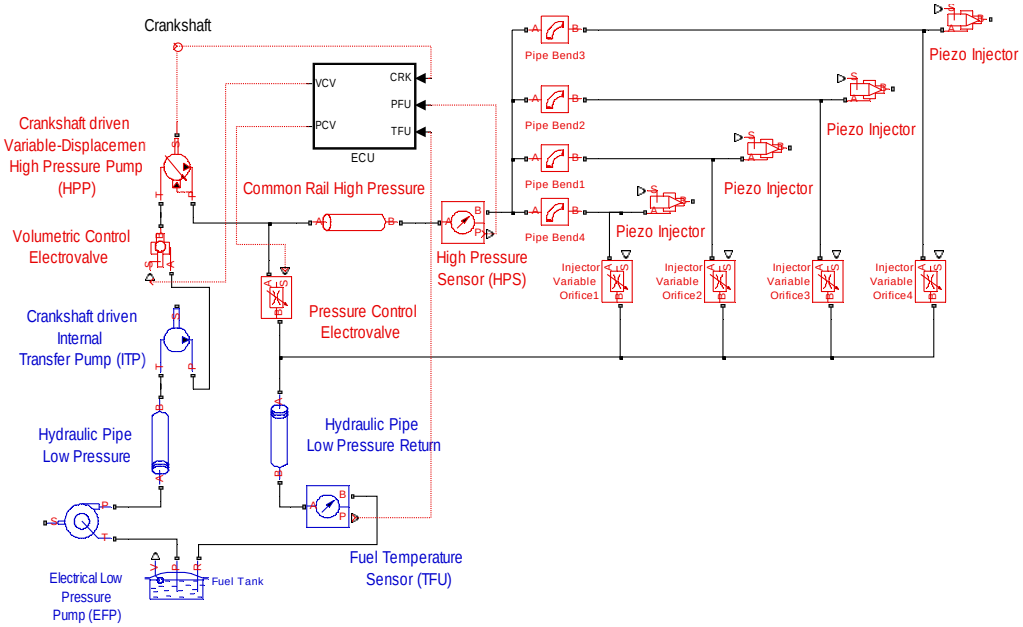

Fig. 2. PCR Hydraulic System.

The fuel pressure set point in PCR is realized via two control loops (fig. 2 – dash lines) implemented using an electronic control unit (ECU) (Continental (2009c)). A first loop, of open-loop type, based on the fuel flow model, is acting on the volumetric control electro-valve, while the second one, of closed loop type, based on the feedback from the fuel pressure sensor, is acting on the pressure control electro-valve. Considering the strong nonlinear characteristics of the process, the control strategies are dependent on the system working point defined as $\Lambda(P,Q,T)$ where P represents the common-rail pressure, Q represents the fuel flow and T the fuel temperature.

The process in the common rail (fig. 3), having as output the common rail pressure P and as control input the flow of fuel eliminated from the high pressure common rail Q_{PCV}, is subject to inherent process disturbances generated by the high pressure pump Q_P, the cumulated flow drop from the injected quantity Q_I, and fuel flow caused by the injector continuous leakage Q_{pl} due to injection affecting the common rail high pressure system.

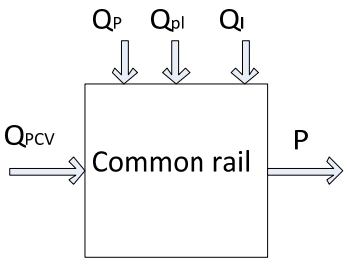

Fig. 3. Schematic representation of high pressure closed loop control with flow contributions to common rail.

Considering the four process inputs as completely separable, the total fuel flow on PCR, $dV/dt = Q_T(t)$, can be expressed as an additive combination:

$Q_T(t) = Q_P(t) + Q_{PCV}(t) + Q_I(t) + Q_{pl}(t)$. Consequently, from relation (1), we have (Gauthier *et al.* 2005):

$$\frac{dP}{dt} = \frac{E(P(t),T(t))}{V_{rail}}\left[Q_P(t) + Q_{pl}(t) + Q_I(t) + Q_{PCV}(t)\right] \qquad (5)$$

where V_{rail} is the rail volume. In (5) each input depends in a specific way on more system variables:

$Q_P(t) = f_P(N(t), \alpha_{CRK}(t), \varphi, \psi_{VCV}(t), \ldots)$, where φ – pump mounting angle, α_{CRK} - crankshaft angle, ψ_{VCV} – volumetric valve opening [%];

$Q_{pl}(t) = f_{pl}(P(t),T)$;

$Q_I(t) = f_{injected\ mass}(Ti,P(t)) + f_{switch\ leakage}(Ti, P(t), T)$, where Ti – time of injection.

$Q_{PCV}(t) = f(\psi_{PCV})$, where ψ_{PCV} – pressure valve opening [%]

It is obvious that the dependencies are more sophisticated than they appear at a first glance because P, as argument, means an implicit feedback connection.

Fig. 4a exhibits a characteristic of common rail fuel pressure P of the system from Fig. 2 when the PCR works around a controlled stationary working point. The shape of P(t) cumulates the effect of all inputs represented in Fig. 3, mainly due to the High Pressure Pump and the Injectors behaviour and the corrective action of the control signal Q_{PCV}. Fig. 4b illustrates the variation of $\alpha_{CRK}(t)$ during the same time interval. The pressure variations P(t) can be correlated to $\alpha_{CRK}(t)$ and associated with the main hydraulic system events (*Continental (2009d)*) during normal engine operation.

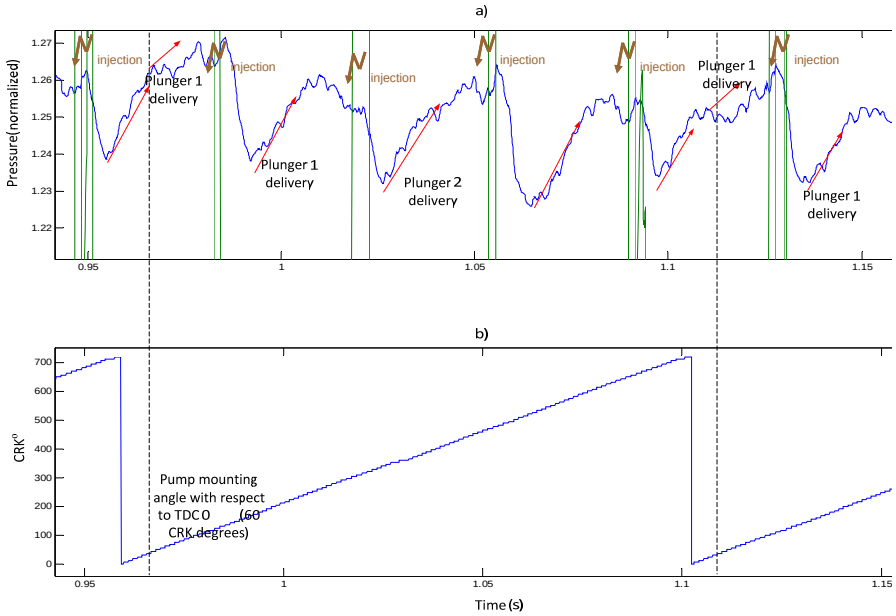

Fig. 4. Measured fuel pressure pattern (a) for a complete engine cycle (720º crankshaft) (b) corresponding to a complete revolution of the 3 Piston Pump (360º crankshaft). Engine speed ~ 800 rpm.

By eliminating time from the dependencies P(t) and $\alpha_{CRK}(t)$, the fuel pressure can be expressed as a function of crankshaft angle $P(\alpha_{CRK})$ (fig. 5 - bottom). For a complete engine cycle (i.e. $\Delta\alpha_{CRK} = 720º$) corresponding to a complete revolution of the 3 pistons pump and to injection realization for all 4 cylinders, the fuel pressure curve can be more clearly correlated with the different hydro-mechanical events (fig. 5 – middle and top): the increase in pressure corresponds to the pump compression time intervals, while the pressure decreasing is linked to injection time intervals.

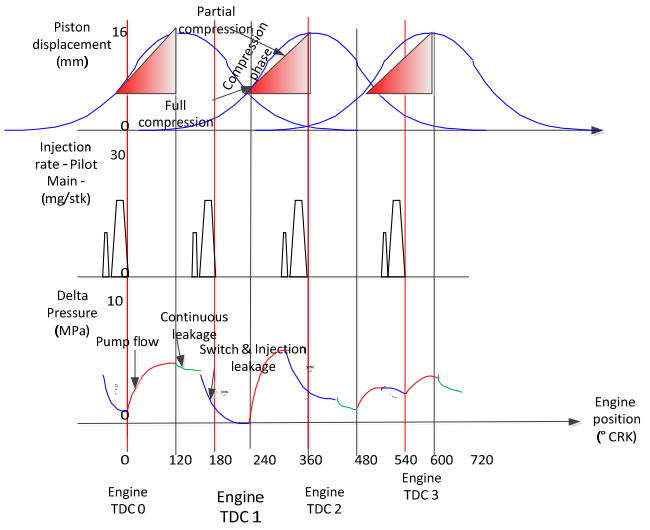

Fig. 5. Idle speed PCR2 characteristic pressure pattern determined by the 3 Piston High Pressure Pump and 4 servo-injectors flow contributions for a full engine cycle (injection configuration: Pilot-Main.

The shapes of the time variations of the disturbances inputs are illustrated in fig. 6. Fig. 6a, represents the pump flow and pressure increase for one piston delivery. Due to mechanical uncertainties, different flow and pressure curves are possible.

Injection events cause flow and pressure drop at certain moments (fig. 6b) while continuous leakage will determine a continuous fuel flow and pressure drop during engine runtime.

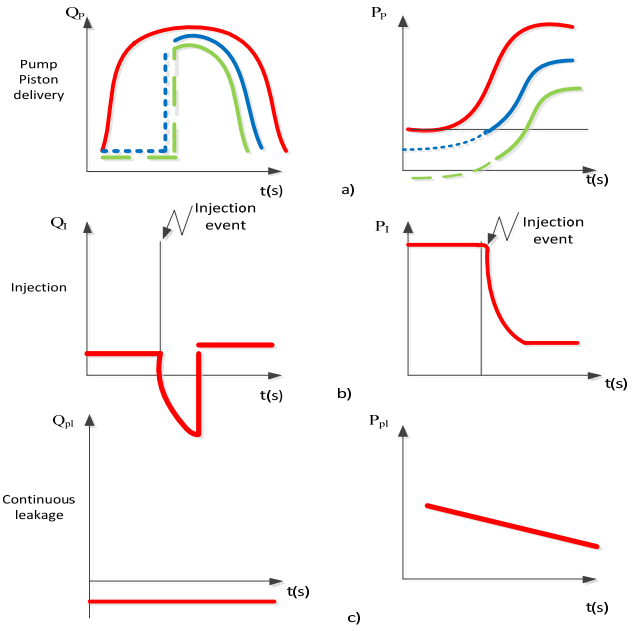

Fig. 6. Theoretical pressure and flow contributions of the PCR system disturbances

After an in-depth quasi-empirical analysis, based on huge amount of practical experiments, similar to those presented above, we have concluded that:

The most important measurable factors, influencing the common rail fuel pressure ($y = P$) behavior in the vicinity of a steady system working point $\Lambda(P,Q,T)$, are: $r=6$, $\underline{u}=[u_1\ u_2\ u_3\ u_4\ u_5\ u_6\ u_7]^T$, where $u_1=\alpha_{CRK}$, $u_2=N$, $u_3=\psi_{PCV}$, $u_4=\psi_{VCV}$, $u_5=v_{inj}$, $u_6=T$ and $u_7=P$. Since Q in common rail is dependent

on *T*, *P*, *N*, ψ_{VCV} and v_{inj}, a split of the input space for different working points can be realized based on the above mentioned variables.

The selection will consist in the following allocations of the variables and preliminary operations: $n_z=5$, $\underline{z}=[z_1\, z_2\, z_3\, z_4\, z_5]^T$ with $z_1=T$, $z_2=P$, $z_3=N$, $z_4=\psi_{VCV}$, $z_5=v_{inj}$; $n_x=4$, $\underline{x}=[x_1\, x_2\, x_3\, x_4]$ with $x_1=f_1(\psi_{PCV})$, $x_2=f_2(v_{\text{inj}})$, $x_3=f_3(\psi_{VCV},N)$, $x_4=f_0(P)=-y$ and $z'=\alpha_{CRK}$. Functions f_0, f_1, f_2 and f_3, have the role of preprocessing the raw variables. The time variable v_{inj}, associated to the injection event and generated by ECU, takes into account the time chart and the flow of injections.

The cyclic system behavior depicted in fig. 5 should be separated depending the pump mounting angle into $n = 6$ evenly distributed regions, called *system phases*, corresponding to pump and injection events where pressure dynamics can be approximated by linear functions. In our case, the phase j, $j = 1,\ldots,6$, covers during a complete revolution the range

$$\alpha_{CRK} \in [60^\circ + 120^\circ (j-1), 180^\circ + 120^\circ (j-1)].$$

In the above mentioned context, the second processing level appears as in Fig.7.

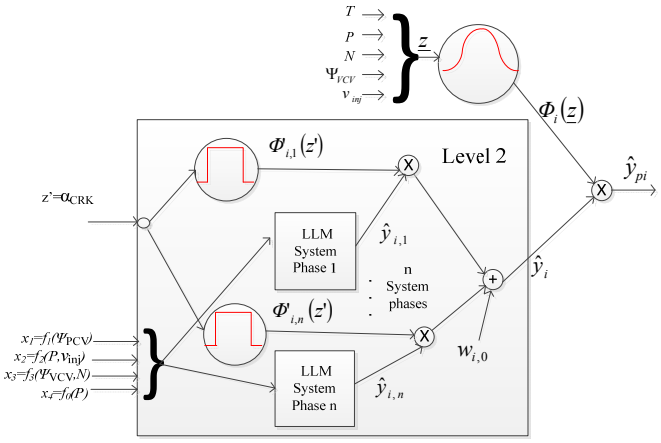

Fig. 7. Neuron consisting in dynamic local model (LMi) used for predicting the common-rail fuel pressure in quasi-stationary working points and associated validity function. The second level realizes the partitioning of the process into linear dynamic linear models corresponding to n system phases for the complete engine cycle (720º crankshaft – 4 cylinders, Pump/Engine ratio = 1/2).

Considering the irregular shape of the disturbances it becomes obvious that approximating the fuel pressure dynamics for different engine working points is not an easy task. Therefore, in order to obtain an accurate model the usage of powerful modeling and identification instruments is necessary.

4. APLICATION STUDY: NEURO-FUZZY ARCHITECTURE DESIGN FOR MODELING AND IDENTIFICATION OF PCR PRESSURE DYNAMICS

Fulfilling the purpose of common-rail fuel pressure modeling and identification, the two level multilayer Neuro-Fuzzy network presented in fig. 1 is proposed. The dynamic local models on level 1 (Fig. 1a) are in fact Neuro – Fuzzy structures themselves as depicted in Fig. 1b and later in Fig. 7. Each dynamic local model (LM_i) consists of n linear local models $LLM_{i,j}$. with $j = 1, \ldots, n$, n being the number of the system phases for a complete engine cycle. The $M \cdot n$ LLMs associated to all M dynamic local models and n phases are chosen to be local optimal ARX predictors of dynamic order m:

$$\hat{y}_{i,j}(k+1|k) = \sum_{l=1}^{n_x-1} B_{i,j,l}(q^{-1}) x_l(k) + \left(1 - A_{i,j}(q^{-1})\right) y(k) \tag{6}$$

where $A_{i,j}(q^{-1}) = 1 + a^1_{i,j} q^{-1} + \cdots + a^m_{i,j} q^{-m}$ and $B_{i,j,l}(q^{-1}) = b^1_{i,j,l} q^{-1} + \cdots + b^m_{i,j,l} q^{-m}$. The coefficients of both operators, i.e. the network's linear parameters, are obtained as solutions of the optimization problem discussed in the next chapter.

The ARX predictors (6) are obtained from ARX models:

$$A_{i,j}(q^{-1}) y(k) = \sum_{l=1}^{n_x-1} B_{i,j,l}(q^{-1}) x_l(k) + e_{i,j}(k) \tag{7}$$

where $e_{i,j}(k) = y(k) - \hat{y}_{i,j}(k \mid k-1)$.

The role of $LLM_{i,j}$ is to predict the dynamic behavior of common-rail pressure for a limited region, "*i,j*", of the input space defined by *z'*. By defining the vector of the weighting operators $\underline{w}_{i,j}(q^{-1}) = [w_{i,j,1}(q^{-1}), \ldots, w_{i,j,nx-1}(q^{-1}), w_{i,j,nx}(q^{-1})]$ with $w_{i,j,l}(q^{-1}) = B_{i,j,l}(q^{-1})$ $(l = 1, \ldots, n_x\text{-}1)$ and $w_{i,j,nx}(q^{-1}) = A_{i,j}(q^{-1})$, equation (6) becomes $\hat{y}_{i,j}(k+1|k) = = \underline{w}_{i,j}(q^{-1})\underline{x}(k)$, where $\underline{x} = [x_1(k), \ldots, x_{nx-1}(k), x_{nx}(k)]^T$. Considering the structure in Fig. 7, follows:

$$\begin{aligned} &\hat{y}_i(k+1 \mid k) = w_{i,0} + \sum_{j=1}^{n} \hat{y}_{i,j}(k+1 \mid k) \cdot \Phi'_{i,j}(z'(k)) = \\ &= w_{i,0} + \sum_{j=1}^{n} \underline{w}_{i,j}(q^{-1}) \underline{x}(k) \cdot \Phi'_{i,j}(z'(k)) \end{aligned} \tag{8}$$

Obviously, the result corresponds to (4). Taking, further, into account the global Neuro – Fuzzy architecture from Fig. 1a, equation (3) is obtained:

$$\begin{aligned} \hat{y}_{pg}(k+1|k) &= \sum_{i=1}^{M} \hat{y}_{pi}(k+1|k) = \sum_{i=1}^{M} \hat{y}_i(k+1|k) \cdot \Phi_i(\underline{z}) = \\ &= \sum_{i=1}^{M} \left[w_{i,0} + \sum_{j=1}^{n} w_{i,j}(q^{-1}) \underline{x}(k) \cdot \Phi'_{i,j}(z'(k)) \right] \cdot \Phi_i(\underline{z}) \end{aligned} \tag{9}$$

The validity functions Φ_i perform a partitioning of the input space associated with premise vector $\underline{z}$ and determine the validity regions "*i*" for the local models in the vicinity of quasi-stationary system working points (ie. idle speed, cruise speed etc).

Some details are now necessary:

- Coefficients from polynomials $A_{i,j}$ reproduce the natural "low pass" characteristics of the process by filtering the measured output signal samples (Nelles, 2001). As $A_{i,j}(q^{-1})$ and $B_{i,j}(q^{-1})$ are polynomials of

order m the global predictor (9) needs $m+1$ samples at the time instants k, $k-1$, …, $k-m$.

- The validity functions $\Phi_{i,j}'(z')$, $j = 1, \ldots, n$ associated to the $LLM_{i,j}$, on level 2, to each phase provide the trust-weights of the $LLM_{i,j}$ outputs in the overall sub-model output to first network level. They are dependent on crankshaft position $z' = \alpha_{CRK}$ and are chosen to be mutual exclusive as suggested in Fig.8 and equation (10):

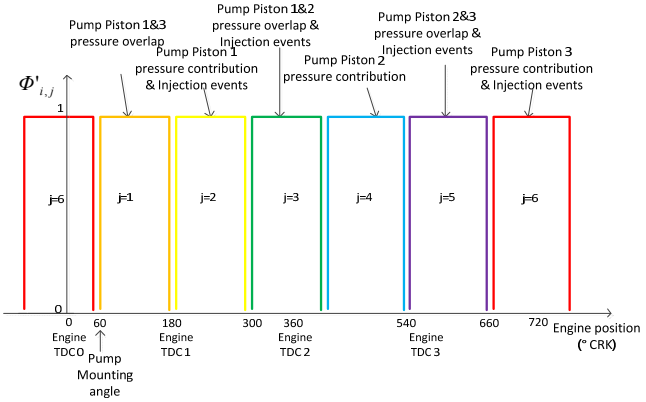

Fig. 8. Validity functions level 2 dependent on crankshaft position for a complete engine cycle (720º crankshaft – 4 cylinders, Pump/Engine ratio = 1/2) , j is the index of phases.

$$\Phi'_{i,j}(z') = \mu'_{i,j}(z'-\alpha_{i,j}) - \mu'_{i,j}(z'-\alpha_{i,j+1}), \tag{10}$$

where $\mu'_{i,j}(\upsilon) = \begin{cases} 0, & \upsilon < 0 \\ 1, & 0 \le \upsilon \end{cases}$, $\alpha_{i,j+1} = \alpha_{i,j} + 120°$, and $\alpha_{i,1} = 60°$.

In equation (9) the validity functions Φ_i form a partition of unity. i.e.:

$$\sum_{i=1}^{M} \Phi_i(\underline{z}) = 1, \tag{11}$$

with

$$\Phi_i(\underline{z}) = \frac{\mu_i(\underline{z})}{\mu_{TOT}(\underline{z})}, \tag{12}$$

where

$$\mu_i(\underline{z}) = e^{-\frac{1}{2}\left(\frac{(z_1-c_{i,1})^2}{\sigma_{i,1}^2} + \cdots + \frac{(z_{nz}-c_{i,nz})^2}{\sigma_{i,nz}^2}\right)}, \tag{13}$$

$$\mu_{TOT}(\underline{z}) = \sum_{j=1}^{M} \mu_j(\underline{z}), \tag{14}$$

and $c_{i,1}, \ldots, c_{i,nz}$ and $\sigma_{i,1}, \ldots, \sigma_{i,nz}$ are the centers, respectively the standard deviation *of region "i"*, representing the network's nonlinear parameters (Nelles, 2001).

5. OFF-LINE PARAMETERS LEARNIG AND MODEL SIMULATION RESULTS

In the Matlab/Simulink application implementing the neuro-fuzzy model presented above, each polynomials $Ai,j,$ and Bi,j,l is of order $m=2$, i.e. 2 coefficients. This choise has two consequences: i) only the information from the last two regressors is used for prediction; ii) $(((m \cdot n_x) \cdot n) \cdot M = 2 \cdot 4 \cdot 6 \cdot M = 48 \cdot M$ coefficients included in weighting operator $\underline{w}_{i,j}(q^{-1})$ should be determined.

In order to determine the model parameters in a real time environment, an on-line LLM parameters adaptation algorithm was implemented in Matlab / Simulink. The coefficients of $\underline{w}_{i,j}(q^{-1})$ are adapted for each prediction sample time k using the recursive least squares algorithm (Nelles, 2001):

$$\begin{aligned} &\underline{\hat{w}}_{i,j}(k) = \underline{\hat{w}}_{i,j}(k-1) + \underline{\gamma}_{i,j}(k) \cdot e_{i,j}(k), \quad e_{i,j}(k) = y(k) - \underline{\tilde{x}}^T(k) \cdot \underline{\hat{w}}_{i,j}(k-1) \\ &\underline{\gamma}_{i,j}(k) = \frac{1}{\underline{\tilde{x}}^T(k)\underline{R}_{i,j}(k-1)\underline{\tilde{x}}(k) + \lambda_i} \underline{R}_{i,j}(k-1) \cdot \underline{\tilde{x}}(k), \\ &\underline{R}_{i,j}(k) = \frac{1}{\lambda_i}\left(\mathrm{I} - \underline{\gamma}_{i,j}(k)\underline{\tilde{x}}^T(k)\right) \cdot \underline{R}_{i,j}(k-1) \end{aligned} \tag{15}$$

where $\underline{R}_{i,j}(k)$ is proportional to the inverse of the covariance matrix of the estimated coefficients $\underline{\hat{w}}_{i,j}(k)^T = \left[\hat{b}^1_{i,j,1}(k) \ldots \hat{b}^m_{i,j,1}(k) \;\cdots\; \hat{b}^1_{i,j,nx-1}(k) \ldots \hat{b}^m_{i,j,nx-1}(k) \;\; \hat{a}^1_{i,j}(k) \ldots \hat{a}^m_{i,j}(k)\right]$ for $LLM_{i,}j$ and $\underline{\tilde{x}}(k)$ represents the normalized extended input vector $\underline{\tilde{x}}(k)^T = \left[\underline{\tilde{x}}_1(k)^T \;\cdots\; \underline{\tilde{x}}_{nx}(k)^T\right]$ where

$$\underline{\tilde{x}}_\ell(k)^T = \left[\underline{\tilde{x}}_\ell(k-1) \;\cdots\; \underline{\tilde{x}}_\ell(k-m)\right], \tilde{x}_\ell(k) = \frac{x_\ell(k) - x_{\ell min}}{x_{\ell max} - x_{\ell min}}, \ell = 1, \cdots, n_x \tag{16}$$

$x_{l\ min}$ and $x_{l\ max}$ are the minimum and maximum values of variable x_l. The algorithm's convergence is considered achieved when all LLM errors $e_{i,j}(k) < 0.2$ %.

For testing the application's tuning capabilities of the predictor, an idle speed working regime was chosen for an experimental vehicle Ford C-max equipped with a 2.0 liter Piezo Common-Rail diesel engine with constant fuel temperature and injection pattern. The nonlinear parameters of the n_z=5 membership functions (13) are given in table 1. Since the experiment is carried out only for idle speed and warm engine and due to small standard deviations for input space variables $\underline{z}$, we considered M = 1, (only one neuron), and, consequently, 48·M=48 coefficients and $\Phi_1(\underline{z})=1$.

The measured data taken from the experimental vehicle was used for training and validation and contains sufficiently excited inputs for the simulation model. The measured signals (table 2) had different ranges and acquisition rates. They were averaged for a 120º CRK (Pump segment) interval to filter out noise and further normalized. Prediction of fuel pressure inherent dynamics is aimed for predictive control so it's necessary to have a sufficiently large prediction horizon

in order to be able to apply the compensation signal in time. Considering for prediction a sample period of 0.025 s, equivalent for an engine rotation of $\Delta\alpha_{CRK}$ = 120º at N = 800 rpm, the model is capable of performing a one step ahead prediction of the fuel pressure behavior allowing a $\Delta\alpha_{CRK}$ = 120º equivalent time window for the process controller to react. The process controller is scheduled to operate with a 0.01 s recurrence.

Table 1. Nonlinear parameters of the membership functions (13) for the idle speed warm engine regime

Membership function μ_i	Linguistic variable z	Centers $c_{i,j}$	Standard deviation $\sigma_{i,j}$
μ_1	z_1= T	$c_{1,1}$=40º C	$\sigma_{1,1}$=0.016
μ_2	z_2= P	$c_{1,2}$=32 MPa	$\sigma_{1,2}$= 0.26
μ_3	z_3= N	$c_{1,3}$=800 rpm	$\sigma_{1,3}$= 6.38
μ_4	$z_4=\Psi_{VCV}$	$c_{1,4}$=24 [%]	$\sigma_{1,4}$=0.9961
μ_5	$z_5=v_{inj}$	$c_{1,5}$=0.56 ms	$\sigma_{1,5}$= 0.032

Table 2. Input Variables

Variable name	Min	Max	Sampling rate
$u_1=\alpha_{CRK}$ = z'	0	720	0.025 s
u_2=N = z_3 (used for x_3)	800	830	0.025 s average
$u_3=\psi_{PCV}$ (used for x_1)	16	17	0.025 s average
$u_4=\psi_{VCV}=z_4$ (used for x_3)	23	25	0.025 s average
$u_5=v_{inj}=z_5$ (also used for x_2)	0	0.77	0.025 s average
u_6=T = z_1	40	41	0.01 s
u_7=P = z_2 (also used for x_4)	31	34.5	0.025 s average

The attribute „average" used in 2 refers to the fact that f_0, f_1 and f_2 reprezents averaging operators that provide at each 0.025 s average values for x_1, x_2 and x_4, denoted above as $x_1(k)$, $x_2(k)$ and $x_4(k)$, obtained from samples of ψ_{PCV}, v_{inj} and P taken during 0.025 s. Function f_3 represents a relation between 0.025 s average N and ψ_{VCV} samples delayed with the time equivalent of 360º CRK with the purpose of correlating the fuel flow inside the pump piston during suction phase.

In the following, it is presented a graphical display of normalized training data (fig. 9 and 10) used for model parameters adaptation. The fuel temperature T (u_6) was kept constant at 40º C. The parameters evolution during adaptation starting from arbitrarily chosen non-zero initial values $\hat{\nu}[0]$ is presented in fig. 11 and the model error in fig. 12. For the adaptation algorithm, the recurrence was identical to the input signals sampling rate. According to figure 11, the estimation process stabilizes and the parameters convergence takes place at about 13 seconds after the training started. The initial values on the diagonal of matrix $\underline{R}_{i,j}$ requires special attention since the convergence of the adaptation algorithm is dependent on those initial values. In case of very high initial values the algorithm is divergent and for very small initial values, the convergence is very slow. In this experiment, the initial values for matrix $\underline{R}_{i,j}$ were chosen to be the identity matrix I_8 multiplied with 0.1. For the forgetting factor λ, influencing the algorithm's convergence speed, the value 0.98 was chosen.

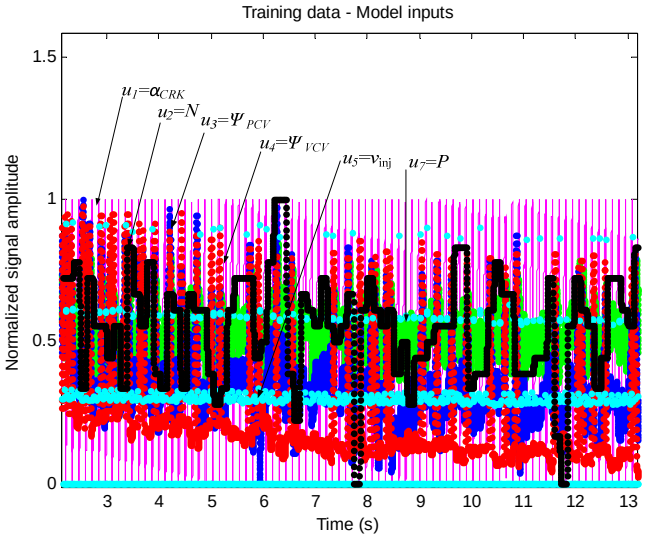

Fig. 9. Normalized training data for LLM parameters adaptation.

For the overall model validation, a comparison between raw value P (0.002 s acquisition rate), 0.025 s average P and the predicted P is presented in fig. 13. The results show a one step ahead prediction of average P with an approximation error less than *1%* which can be considered satisfactory considering the constraints imposed in the introductive section of this paper.

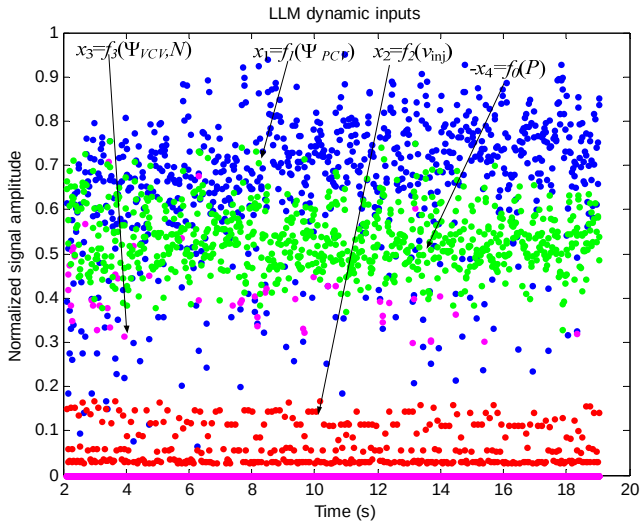

Fig. 10. LLM dynamic inputs normalized

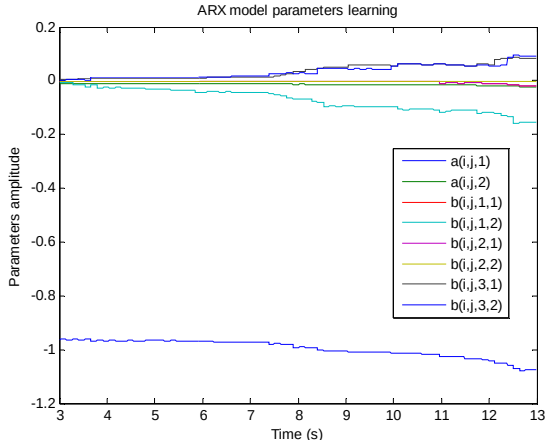

Fig. 11. LLMi,j parameters evolution during adaptation.

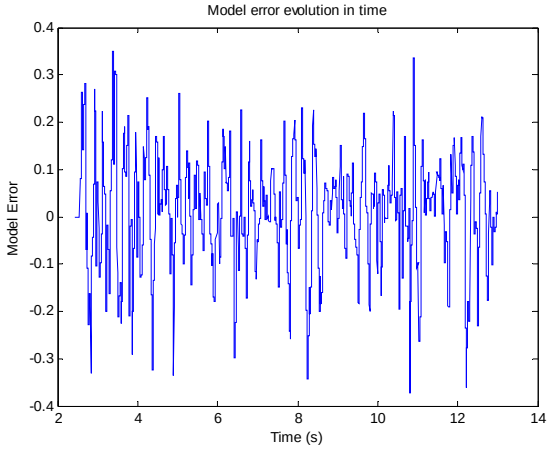

Fig. 12. Overall model error evolution during training phase.

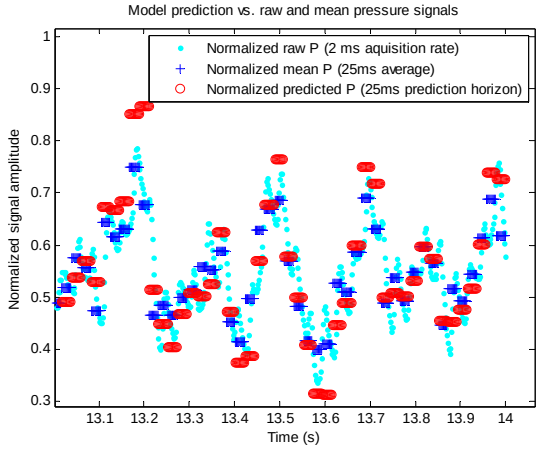

Fig. 13. Graphical comparison of measured fuel pressure signal P (2 ms acquisition rate), mean P used for model training and model predicted P.

5. CONCLUSIONS AND PERSPECTIVES

Following the analysis of common-rail diesel hydraulic system, different factors were identified to be responsible of fuel pressure shaping and they were classified accordingly. Considering the complexity of the technological process, a solution for offline and on-line modeling and identification was implemented using fast Neuro-Fuzzy networks. These type of structures, capable to classify the operating modes of the system and to approximate them for the entire engine operating regimes, are the perfect candidates for satisfying the exigent requirements regarding performance and reliability.

A small scale application, implementing the common rail prediction model and parameters adaptation, is already showing promising results. The adaptation of model parameters can be performed in a reasonable timeframe. The prediction of common rail fuel pressure can be preformed around a quasi-stationary engine working point with deviations under 1 MPa. Further design of the system identification structure will emphasize on generality and real time performance. An input space decomposition algorithm will determine the number of rules and neurons necessary for achieving good prediction performances for all engine working points. Along with the performance criteria, the model design will incorporate constrains related to memory usage and runtime. Once implemented, the common rail prediction model opens perspectives for model based predictive control.

ACKNOWLEDGMENT

Many thanks to Continental Powertrain Engine System for the technical support.

This work was partially supported by the strategic grant POSDRU/88/1.5/S/50783, Project ID50783 (2009), co-financed by the European Social Fund – Investing in People, within the Sectorial Operational Program Human Resources Development 2007-2013.

REFERENCES

Boudy, F., Seers, P., (2009). Impact of physical properties of biodiesel on the injection process in a common-rail direct injection system, *Energy Conversion and Management*, 50, p. 2905 – 2912.

Continental (2009a), *Euro 6 and CO2 reduction: New technologies to meet the challenges of the coming years*. Available from: http://www.conti-online.com/generator/www/com/en/continental/pressportal/themes/press_releases/3_automotive_group/powertrain/press_releases/pr_2009_09_15_euro_6_en.html [Accessed: August 31, 2012].

Continental Automotive GmbH, Adler C. *et al*, (2009b). *Kraftstoffdruckregelsystem*, Pat. DE102007060006B3.

Continental Automotive GmbH, Li, H., (2009c). *Superimposed pressure of the commonrail system*, Pat. WO/2009/ 132898.

Continental Automotive GmbH, Jung, U., Radeczky J., Wirkowsky, M., (2009d). *Method for determining the rail pressure in a common rail system and common rail injection system*, Pat. WO/2009/132898.

Delphi (2009), *Delphi Common Rail Fuel Systems*. Available from: Web site: http://delphi.com/manufacturers/auto/powertrain/diesel/crfs/ [Accessed: August 31, 2012].

Gauthier C. et al., (2005). Modeling of a diesel engine common rail injection system, *Proceedings of the 16th IFAC World Congress*.

Hafner, M., Schuler, M. and Nelles, O. (2002). Neural net models for diesel engines- simulation and exhaust optimization*, Control Engineering Practice*, Vol. 30, No. 2, pp. 402-412.

Jakubek S., Keuth N., (2006). A local neuro-fuzzy network for high-dimensional models and optimization. *Engineering Applications of Artificial Intelligence*, 19, p. 705–717.

Kiijarvi, J., (2003). Diesel fuel injection system simulation, *Publications of the Internal Combustion Engine Laboratory*, Helsinki University of Technology, No. 77, 126 pp. ISBN 951-22-6657-1, ISS1459-5931.

Lino P., Maione B., Rizzo A., (2007), Nonlinear modeling and control of a common rail injection system for diesel engines, *Applied Mathematical Modeling*, 31 (9), pp. 1770-1784.

Lino P., Maione B., Amorese C.,(2008). Modeling and predictive control of a new injection system for compressed natural gas engines, *Control Engineering Practice*, 16, 1216–1230.

Murray-Smith R., (1994). A local model network approach to nonlinear modeling. *Ph.D. Thesis*, University of Strathclyde, UK.

Nelles O., Fischer M., (1996). Local linear model trees (LOLIMOT) for nonlinear system identification of a cooling blast", *European Congress on Intelligent Techniques and Soft Computing (EUFIT)*, Aachen, Germany.

Nelles, O., Isermann, R., Fink, A., (2000). Local linear model trees (LOLIMOT) toolbox for nonlinear system identification, *12th IFAC Symposium on System Identification,* (SYSID), Santa Barbara, USA.

Nelles, O., (2001). *Nonlinear system identification*, chapter 14, Springer-Verlag, ISBN 3-540-67369-5.

Seykens, X.J.L., Somers, L.M.T. & Baert, R.S.G., (2004). Modeling of common rail fuel injection system and influence of fluid properties on injection process. *Proceedings of VAFSEP*, Dublin, Ireland.

Wikipedia (2012), Common rail. Available from: Wikipedia, Web site: http://en.wikipedia.org/wiki/Common_rail [Accessed: August 31, 2012].

Yldiz Technical University (2009). Available from: Yldiz Technical University, Web site: http://www.yildiz.edu.tr/~oisin/Dersler/Dersnotlari/0653611/dinjection.pdf [Accessed: August 31, 2012].

Zeliang, Li., (2005). Condition monitoring of axial piston pump, *Master of Science Thesis*, University of Saskatchewan, Saskatoon, Canada.

Zhang Z., Sun Z., (2009). "Rotational Angle Based Pressure Control of a Common Rail Fuel Injection System for Internal Combustion Engines", *American Control Conference Hyatt Regency Riverfront*, St. Louis, MO, USA.